

## Optical properties of CrSb, MnSb, NiSb, and NiAs

J. W. Allen and J. C. Mikkelsen

Xerox Palo Alto Research Center, Palo Alto, California 94304

(Received 4 October 1976)

The room-temperature optical reflectivity of metallic CrSb, MnSb, NiSb, and NiAs has been measured between 0.05 and 5.0 eV, and the optical constants have been deduced by a Kramers-Kronig analysis. The nickel compounds have a low-energy region of intraband character while CrSb and MnSb show strong interband transitions to the lowest energy measured. This is interpreted as supporting a band model in which there are  $3d$  states at the Fermi level for MnSb and CrSb, but not for nickel compounds. The departures of the intraband optical properties of the nickel compounds from Drude behavior are described by a generalized Drude analysis in terms of a complex energy-dependent lifetime, the real part of which has an approximate  $\omega^2$  dependence.

### I. INTRODUCTION

This paper reports measurements of the room-temperature optical reflectivity of CrSb, MnSb, NiSb, and NiAs in the energy range 0.05–5 eV, and the optical constants derived from the data by a Kramers-Kronig analysis. These results are interpreted as supporting a metallic-energy-level model proposed previously<sup>1,2</sup> and described briefly below. In addition, a quantitative analysis of the intraband optical constants of NiSb and NiAs is given, using an extension of a method suggested by Hopfield.<sup>3</sup>

In making energy-level models for transition metals and their compounds, it is often uncertain whether the  $3d$  electrons should be regarded as localized or itinerant and whether the occupied  $3d$  states are energetically isolated or overlapping with other states. Within this framework there are four general possibilities: (a) isolated-localized, (b) isolated-itinerant, (c) overlapping-localized, and (d) overlapping-itinerant. For Mott insulators like Cr<sub>2</sub>O<sub>3</sub>, (a) appears to be appropriate with "localized" understood in the Mott-Hubbard sense, and the  $3d$  states energetically isolated in a bonding-antibonding gap between filled anion  $p$  states and empty metal  $4s$  states.<sup>4,5</sup> For paramagnetic, metallic V<sub>2</sub>O<sub>3</sub> the occupied  $3d$  states are thought to be isolated as in Cr<sub>2</sub>O<sub>3</sub>, but bandlike as in model (b).<sup>4,5</sup> For the transition metals there is energetic overlap of  $3d$  states and  $4s$  bands, and there has been debate<sup>6</sup> as to whether (c) or (d) or some hybrid model<sup>7</sup> is appropriate.

Obtaining definitive experimental evidence favoring one model or the other has been difficult (possibly because each model lacks some essential features). Efforts at distinguishing models have tended to focus on the question of "localized" or "itinerant," and this subject is discussed at length by Herring,<sup>6</sup> Goodenough,<sup>4</sup> and others. In contrast, the issue of "overlapping" or "isolated" has not arisen so often and is not much discussed. But it

is an important question in picking an energy-level model for the transition-metal pnictides in general and antimonides in particular.

The compounds discussed in this paper all have the NiAs structure and are metallic. CrSb orders antiferromagnetically, MnSb orders ferromagnetically, and NiSb and NiAs are either diamagnetic or very weakly paramagnetic. In an ionic-bonding model the anion would have filled  $p$  states, the  $3d$  states would be occupied with a number of electrons corresponding to a metal  $3^+$  ion, and the Fermi level would intersect only  $3d$  states. Since the materials are metals, model (b) would be implied. A transition to models of type (c) or (d) occurs if the bonding is imagined to be less ionic and more metallic to the extent that the  $3d$  states overlap the anion  $p$  states with the Fermi level lying in the overlap region. Then the anion  $p$  states are only partly filled and the  $3d$  states have an occupancy greater than that corresponding to a metal  $3^+$  ion. Although an itinerant picture for the  $3d$  electrons is no longer required by the metallic conductivity, since the Fermi level intersects anion  $p$  states, it is strongly suggested by the noninteger magnetic moments observed and is here assumed to be appropriate. Thus, it is desired to distinguish between models of type (b) and (d). At present, band theory often does poorly in predicting the relative positions of the anion and cation states, so it is important to settle the question experimentally. Although photoemission experiments presently provide the most-direct experimental information, there remain some uncertainties in their interpretation, and so it is worthwhile also to use other methods such as optical spectroscopy. In the paragraphs below, it is argued that the differences in the reflectivity of the various compounds can be used to test a model.

The metallic model resembles the one commonly accepted for transition metals in having the Fermi level fall in a region where narrow  $d$  bands inter-

sect and hybridize with broader bands. This model was proposed for MnSb, motivated by a great similarity of its experimental properties to those of magnetic transition metals.<sup>1</sup> The existence of  $p$ - $d$  overlap at the Fermi level appears to be confirmed by recent x-ray photoemission experiments.<sup>8</sup> The model has been extended to other transition-metal antimonides by assuming that, as with the transition metals, the  $3d$  bands decrease in energy and become narrower in the sequence from Ti to Ni. This picture works quite well in providing a qualitative interpretation of the properties of the antimonides.<sup>2</sup> For example, the  $3d$  states should be very nearly filled in NiSb (and NiAs), which is quite consistent with the fact that these compounds are weakly magnetic.

In the case of the optical properties, a similarity of MnSb to a transition metal was found in that the reflectivity falls from 100% immediately as the energy increases from zero in the infrared, and decreases more slowly with very little structure on through the visible, producing a somewhat dull silvery appearance. This behavior contrasts with that of silver where the reflectivity is near 100% throughout the infrared and visible. For the transition metals the low-energy fall of the reflectivity is generally ascribed to the influence of numerous low-energy interband transitions which occur because of the high density of  $3d$  states at the Fermi level.<sup>9</sup> Such processes do not occur for silver until 4 eV because the  $3d$  states are filled and located that amount of energy below the Fermi level. Similarly, copper derives its color from a reflectivity edge at 2 eV due to  $3d$  states 2 eV below the Fermi level. Thus the model of the preceding paragraph implies that another magnetic antimonide like CrSb will have a dull silvery appearance, and that the nickel compounds could be colored metals if their  $d$  states are filled. Preparing the compounds showed this to be the case. CrSb is dull silver, NiAs is yellow, and NiSb is light pink. However, measuring the reflectivity showed the color of the nickel compounds to be due to a second reflectivity edge, the first occurring at about 0.5 eV. The first edge is taken to indicate that the  $3d$  states in NiSb and NiAs are only slightly below the Fermi level.

The qualitative picture of the preceding paragraphs has been presented briefly elsewhere.<sup>10</sup> Section II of this paper gives a more complete presentation of the experimental results for the antimonides, including those for NiAs, which have not been presented before. Section III gives as detailed an interpretation of the data as is presently possible. This includes a quantitative discussion of departures of the intraband results for NiSb and NiAs from Drude behavior. The intraband analysis

utilizes an extension of a method given by Hopfield<sup>3</sup> and the extension is described in the Appendix. Section IV provides some perspective on the interpretation.

## II. EXPERIMENTAL

The samples of CrSb, NiSb, and NiAs were prepared by a vertical Bridgman-Stockbarger method, and samples of  $Mn_{1-x}Sb$ , obtained from Chen, were grown by Czochralski pulling from an Sb-rich melt.<sup>1</sup> Sample faces were exposed by cutting with a diamond saw and were mechanically polished. The reflectivity measurements were made at room temperature. In the energy range 0.05–0.5 eV, the reflectivity was measured with a Perkin-Elmer 180 spectrometer. Between 0.5 and 5 eV, data were taken point by point using an experimental system which consisted of a reflectometer with an optical design similar to that described by Feinleib and Feldman,<sup>11</sup> a Spex 1302 monochromator, a cooled PbS detector, a cooled RCA C31034A photomultiplier tube, a water-cooled tungsten-halogen lamp, and a deuterium lamp. For all the data reported here, the sample faces were not oriented and the light was unpolarized. One oriented MnSb sample was prepared so that  $\sigma$  and  $\pi$  spectra could be taken and no significant difference between the two spectra was found in the energy range 0.05–0.5 eV. The data from the two systems generally showed a mismatch at 0.5 eV of (1–4)% and the 0.5–5-eV data were scaled to the 0.05–0.5-eV data to produce a smooth composite spectrum. The data thus obtained for the four compounds are shown in Figs. 1 and 2. For  $Mn_{1-x}Sb$ , four samples with  $0.013 < x < 0.15$  were studied. The data were nearly independent of  $x$  for the four samples and only the data for the most stoichiometric sample are shown.

A Kramers-Kronig analysis was used to obtain optical constants from the reflectivity data. In the

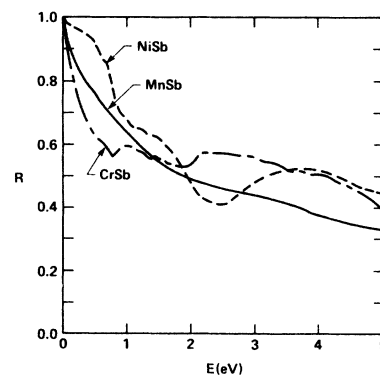


FIG. 1. Unpolarized room-temperature optical reflectivity of CrSb, MnSb, and NiSb.

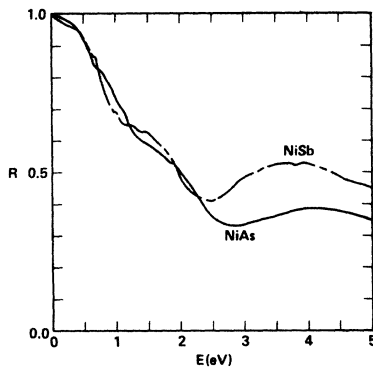


FIG. 2. Unpolarized room-temperature optical reflectivity of NiSb and NiAs.

range 0.05–0 eV, the data were extrapolated by hand smoothly to a reflectivity of 1.0. Above 180 eV, the reflectivity was set to zero. Between 5 and 180 eV several extrapolations were tested. These included setting the reflectivity to zero at 5 eV, and also using  $R(\epsilon) = R(5 \text{ eV})(\frac{1}{5}\epsilon)^n$  for various  $n$  between  $-4$  and the unphysical value 2. The net effect of all the different schemes is to float the optical constant spectra up and down by factors of 2 or 3, but not to change the spectral structure. For the purposes of this paper, the uncertainty in the actual values of the optical constants is unimportant. The computer program employed for the analysis is essentially identical to the one used by Bauer *et al.*<sup>12</sup> The optical conductivities and dielectric constants thus obtained are shown in Figs. 3–6.

A modest effort was made to apply the oscillator fit method in analyzing the reflectivity data using an extensive set of established computer programs.<sup>13</sup> The rather featureless character of much of the data made it difficult to fit with small numbers of oscillators, and this method did not appear

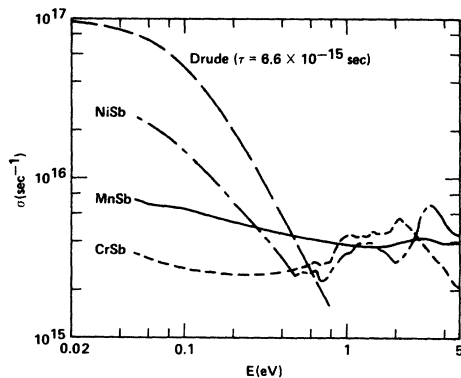


FIG. 3. Optical conductivity of CrSb, MnSb, and NiSb.

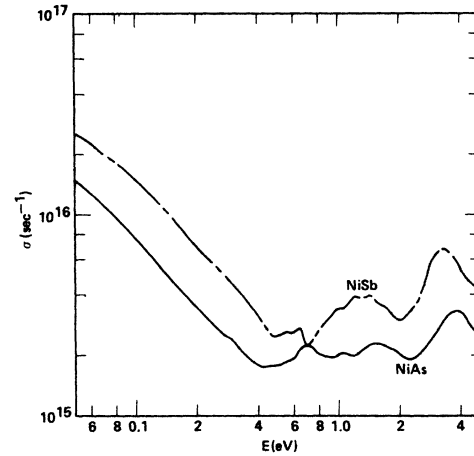


FIG. 4. Optical conductivity of NiSb and NiAs.

especially advantageous relative to the Kramers-Kronig analysis for the data at hand.

### III. DATA INTERPRETATION

#### A. Intradband region

As mentioned in Sec. I, there is a qualitative difference between the nickel compounds and the two

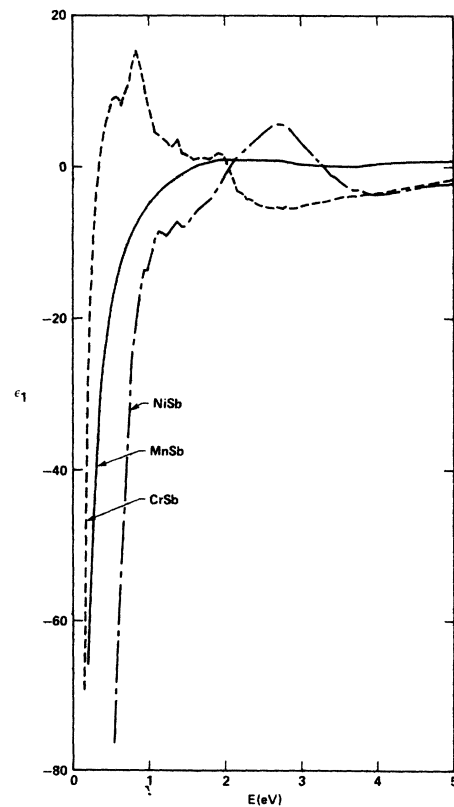


FIG. 5. Dielectric constant of CrSb, MnSb, and NiSb.

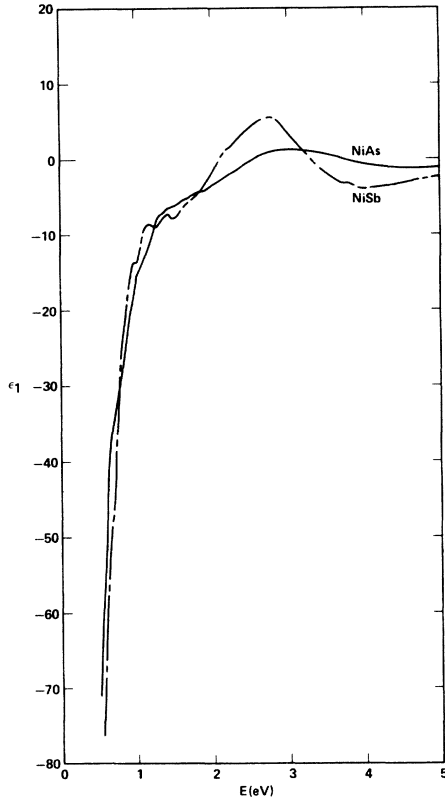


FIG. 6. Dielectric constant of NiSb and NiAs.

other materials. This difference can be seen by comparing the various optical conductivity curves of Figs. 3 and 4. Figure 3 gives a plot of the Drude intraband conductivity from Eq. (1) [see Eq. (A1)]:

$$\sigma(E) = \frac{\omega \epsilon_2}{4\pi} = \frac{\omega_p^2 \tau / 4\pi}{1 + (E\tau/\hbar)^2} \quad (1)$$

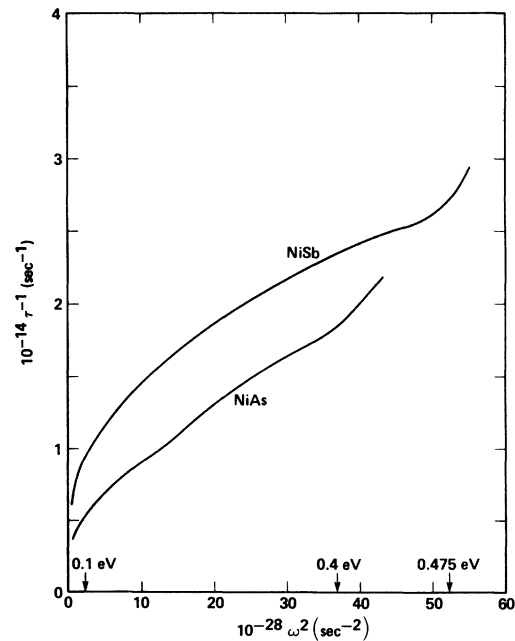
for  $\sigma_0 = \omega_p^2 \tau / 4\pi = 10^{17} \text{ sec}^{-1}$  and  $\tau = 6.6 \times 10^{-15} \text{ sec}$ . On a log-log plot like Fig. 3, Drude curves for other values of  $\sigma_0$  and  $\tau$  are obtained by vertical and horizontal translations of the curve shown. It is evident that up to 0.5 eV the nickel compounds' conductivities have a low-energy region of definite intraband character, although they will not be fit by the simple Drude expression of Eq. (1). For MnSb and CrSb, however, it is clearly not meaningful to describe any portion of the spectrum as intraband in character. This is here interpreted as implying that these two compounds have numerous low-energy interband transitions which are absent in the nickel compounds until the rather sharp cutoff of intraband character at about 0.5 eV. As pointed out in Sec. I this difference is very much consistent with the energy-band model described there.

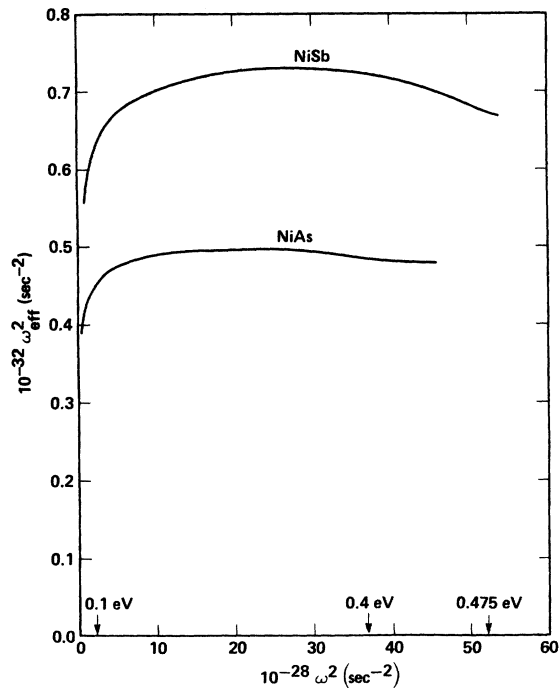
The departure of the conductivities of the nickel

compounds from simple Drude behavior can be partly ascribed to a smooth continuation of interband processes below 0.5 eV, but the size of this tail is not large enough to account for all the differences. It is generally appreciated that departures from Drude behavior are expected for metals with *d* states at or near the Fermi level because the scattering processes are too complex to be described by the simple relaxation-time ansatz leading to the Drude formula.

It might be thought that these departures could be accounted for by letting  $\tau$  in Eq. (1) be frequency dependent to fit the data, and in fact the data of Fig. 4 can be described fairly well by letting  $1/\tau = a + b\omega^2$ . But the discussion in the Appendix shows that this is not a correct procedure and that both  $\tau$  and  $\omega_p^2$  must be given a frequency dependence, as defined by Eqs. (A2) and (A3), to keep the Drude form and have  $\tilde{\epsilon}$  be causal. It is also shown that both frequency dependences arise simultaneously, and can be given in terms of *R* and *I*, the real and imaginary parts, respectively, of a causal function *G*, which characterizes scattering in the collision term of the Boltzmann equation.

Figures 7 and 8 show  $1/\tau_{\text{eff}}$  and  $\omega_{\text{eff}}^2$  for NiAs and NiSb. The quantities are plotted versus  $\omega^2$ , motivated by the discussion centered around Eq. (A11). For both, but more clearly for NiAs, in the range from the intraband cutoff down to about 0.1 eV  $\omega_{\text{eff}}^2$  is roughly constant and  $1/\tau_{\text{eff}}$  has a very approximate  $\omega^2$  dependence. But below 0.1 eV, especially for NiSb, the slope of  $1/\tau_{\text{eff}}$  changes and

FIG. 7.  $1/\tau_{\text{eff}}$  for NiSb and NiAs.

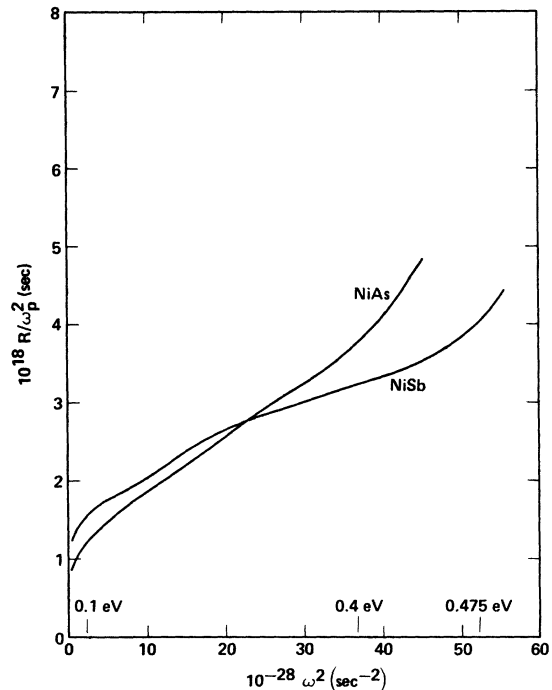
FIG. 8.  $\omega_{\text{eff}}^2$  for NiSb and NiAs.

$\omega_{\text{eff}}^2$  decreases sharply. Figure 9 shows  $R/\omega_p^2$ , computed using Eq. (A11). The approximate  $\omega^2$ -dependence is qualitatively better for  $R$  than for  $1/\tau_{\text{eff}}$  and the low-energy tailing off is reduced. This shows that the effects of  $I(\omega)$  and  $R(\omega)$  should be separated. It is well to remember that the shapes in the energy range 0.05–0.10 eV may be sensitive to the low-energy extrapolation used in the reflectivity, and are therefore less significant. This is particularly true since  $\epsilon_1$  and  $\epsilon_2$  have very large magnitudes and change very rapidly with energy in this range. In view of this, it seems fair to state that an approximate  $\omega^2$  dependence of  $R(\omega)$  has been found.

If it is assumed for the moment that  $(1-I/\omega)$  is approximately 0.5 to 1, then  $\omega_{\text{eff}}^2$  gives an estimate of  $\omega_p^2$ . For NiAs, using Fig. 8,  $\omega_p^2$  is about  $0.5 \times 10^{32} \text{ sec}^{-2}$ , so the plasma energy is about 4.7 eV. From Fig. 9, it then follows that for NiAs  $R(\omega)$  is approximately

$$R(\omega) \cong 0.5 \times 10^{14} + 5 \times 10^{-16} \omega^2. \quad (2)$$

The result for NiSb is very similar. If  $I(\omega)$  has a magnitude comparable to the frequency-dependent part of  $R$ , the assumption about  $(1-I/\omega)$  above will be met. The coefficient of  $\omega^2$  in  $R(\omega)$ , called  $b$  by Hopfield, has the order of magnitude estimated by Hopfield for several mechanisms, one being electron-electron scattering. It is interesting to note that this is about 100 times larger than the esti-

FIG. 9.  $R(\omega)/\omega_p^2$  for NiSb and NiAs.

mate of Gurzhi, as discussed by Thèye,<sup>14</sup> for electron-electron scattering.

The final point of this subsection is to note that the dc conductivity of  $\text{Mn}_{1-x}\text{Sb}$  decreases by more than a factor of 2 as  $x$  changes from 0.013 to 0.152,<sup>1</sup> and that this change is not displayed at all in the infrared reflectivity. If the optical conductivity in the energy range measured is due primarily to interband transitions, rather than intraband transitions, as suggested here, then this is not surprising. Another consideration is that the scattering mechanism introduced by the interstitial manganese atoms may be more important for states very near the Fermi surface than for states probed in the optical measurement.

#### B. Interband region

Figures 3 and 4 show that the interband transitions of NiSb and NiAs are similar, but that otherwise there is little correlation in the spectra of the different compounds. In the absence of a band-structure calculation, it is difficult to be very detailed in assigning the optical structure. It seems likely that transitions to and from  $d$  states will dominate since the density of  $d$  states is the largest. There is some correlation of the peak positions for the nickel compounds and CrSb with those of the elemental metals.<sup>15</sup>

For the nickel compounds, with the band model of this paper, the structure could reflect the den-

sity of  $d$  states downward from the Fermi level, implying a total  $d$ -band width of about 5 eV. It might be anticipated that this density of states would be basically bimodal due to the cubic crystal field (as in the cubic transition metals), with some additional structure because the crystal is uniaxial and has two formula units per unit cell. This picture is generally consistent with the structure observed. The interband threshold for NiAs occurs at a slightly lower energy than in NiSb, implying the  $d$  states are closer to the Fermi level in NiAs.

For MnSb, the lack of structure permits only the observation that of all the transition metals, manganese has the least optical structure<sup>15</sup> and is much like MnSb. CrSb contrasts with MnSb in having more spectral structure. The structure is different from the nickel compounds and this is expected since the  $d$ -state filling is much different. The actual shape will depend in detail on the antiferromagnetic band structure of CrSb.

Figures 5 and 6 show the very strong interplay of interband and intraband transitions in these materials. The slope of  $\epsilon_1$  is quite steep at the initial zero crossing, especially for CrSb, and this is because the positive contribution of interband transitions to  $\epsilon_1$  causes the zero crossings to occur at lower energies than would be the case with only the intraband transitions. The lack of very-low-energy interband transitions in the nickel compounds, as compared to MnSb and CrSb is also very apparent, and allows the zero crossing of  $\epsilon_1$  for the nickel compounds to occur at higher energies.

#### IV. DISCUSSION

This paper has interpreted the optical properties of four transition-metal compounds from the viewpoint of a particular qualitative band-structure model. It would be naive at this stage of understanding of these materials to expect that no other interpretation could be given. As mentioned in the introduction, an alternative picture for these materials is that the anion  $p$  states are filled and that the  $d$  state occupation is similar to that of metal  $3^+$  ion. It would then be argued that the nickel compounds are weakly magnetic because their  $d$  bands are too broad to support magnetic moments. A possible example of a compound that fits this description is  $\text{LaNiO}_3$ .<sup>16,17</sup> Then it might be consistent with the optical data presented here to argue that the breadth of the  $d$  states is such that the interband threshold occurs at a high enough energy to permit an intraband region. It would be very interesting to compare the intraband optical constants of  $\text{LaNiO}_3$  with those reported here for NiAs and NiSb, but unfortunately,  $\text{LaNiO}_3$  has not been measured.

It is relevant in this connection to note that there is some evidence that magnetic transition metals (with unfilled  $d$  states) do have interband thresholds in the energy range 0.1–0.5 eV,<sup>18</sup> as do the nickel compounds discussed here. However, the interband thresholds do not vary in a systematic way across the transition metal sequence, even though the  $d$ -band widths do, and no qualitative difference occurs until copper, with its filled  $d$  states, is reached. For the magnetic antimonides, the interband thresholds occur at much lower energies than for the magnetic transition metals, and there is a distinct qualitative difference for the nickel compounds. Thus, in the interpretation of this paper, it is the *change* in the interband threshold from compound to compound, rather than the actual value, that is regarded as significant.

To summarize, this paper has presented the first optical data on NiAs, NiSb, MnSb, and CrSb. The data have been interpreted as supporting a metallic-energy-band model characterized by  $d$ -state occupations close to those of a transition metal. In addition, the departures of the intraband optical constants of NiSb and NiAs from Drude behavior have been analyzed quantitatively using a generalized Drude analysis, and an approximate  $\omega^2$  dependence for the real part of the complex lifetime has been demonstrated.

#### ACKNOWLEDGMENTS

We gratefully acknowledge the aid of G. Lucovsky and W. Y. Liang in obtaining the infrared data, the excellent technical assistance of R. Allen in obtaining the visible data, and helpful discussions with R. M. Martin.

#### APPENDIX: GENERALIZED DRUDE ANALYSIS

In Sec. II, the interpretation of the data in the intraband region is discussed. As a basis for the discussion it is convenient to make some useful general observations which have not appeared explicitly elsewhere.

Modest departures of the intraband optical properties of metals from the Drude dielectric-constant formula

$$\begin{aligned} \bar{\epsilon} - \epsilon_\infty &= \frac{-\omega_p^2}{\omega(\omega + i/\tau)} \\ &= \frac{-\omega_p^2}{\omega^2 + 1/\tau^2} + i \frac{\omega_p^2}{\omega\tau(\omega^2 + 1/\tau^2)} \end{aligned} \quad (\text{A1})$$

are often accounted for by the plausible scheme of ascribing a frequency dependence to the lifetime  $\tau$ . There have been two approaches to this. One, used by Th  ye,<sup>14</sup> is to choose  $\tau(\omega)$  to make the imaginary part of Eq. (A1) fit the experimental  $\epsilon_2$ . Another,

suggested by Hopfield,<sup>3</sup> is to observe that Eq. (A1) implies the relation (neglecting  $\epsilon_\infty$ )

$$1/\tau = -\omega\epsilon_2/\epsilon_1 \quad (\text{A2})$$

and to use Eq. (A2) as a definition of  $\tau_{\text{eff}} = \tau(\omega)$ , to be evaluated for an experimental  $\epsilon_1$  and  $\epsilon_2$ . These two procedures are not generally equivalent. This is because Eq. (A1) with  $1/\tau = 1/\tau(\omega)$  has poles in the upper-half complex  $\omega$  plane, as well as the lower-half, and thus is not causal, even for such a gentle  $\omega$  dependence as  $1/\tau = a + b\omega^2$ . Therefore, an experimental  $\epsilon_1$  and  $\epsilon_2$ , which satisfy the Kramers-Kronig relations, cannot be fit by the real and imaginary parts of Eq. (A1) with the same  $\tau_{\text{eff}}$ . To obtain a causal  $\bar{\epsilon}$  with the Drude form, it is necessary to let  $\omega_p^2$  be frequency dependent also. If Eq. (A2) defines  $\tau_{\text{eff}}$ , then the real part of Eq. (A1) leads to a definition of an effective  $\omega_p^2$ :

$$\omega_{\text{eff}}^2 = (-\epsilon_1)(\omega^2 + 1/\tau_{\text{eff}}^2). \quad (\text{A3})$$

The frequency dependence of  $\omega_{\text{eff}}^2$  removes non-causal poles introduced by  $\tau_{\text{eff}}$  into  $\bar{\epsilon}$ .

The frequency dependence of  $\omega_p^2$  and  $\tau$  arise simultaneously on the microscopic level. This can be seen most easily, if not most rigorously, by considering how a Drude conductivity with frequency-dependent  $\tau$  might arise from the Boltzmann equation. The linearized Boltzmann equation for the departure  $g_{\mathbf{k}}$  of the distribution function of the state  $\mathbf{k}$ ,  $f_{\mathbf{k}}$ , from its equilibrium value  $f_{\mathbf{k}}^0$  due to an applied electric field  $\vec{E}$  is<sup>19</sup>

$$e\vec{E} \cdot \vec{v}_{\mathbf{k}} \left( -\frac{\partial f_{\mathbf{k}}^0}{\partial \mathcal{E}} \right) = -\frac{\partial f_{\mathbf{k}}}{\partial t} \Big|_{\text{col}} + \frac{\partial g_{\mathbf{k}}}{\partial t}. \quad (\text{A4})$$

To obtain a frequency-dependent  $\tau$ , the collision term can be generalized from the relaxation-time ansatz

$$-\frac{\partial f_{\mathbf{k}}}{\partial t} \Big|_{\text{col}} = \frac{1}{\tau} g_{\mathbf{k}} \quad (\text{A5})$$

to the form

$$-\frac{\partial f_{\mathbf{k}}}{\partial t} \Big|_{\text{col}} = \int_{-\infty}^t g(t-t')g_{\mathbf{k}}(t') dt'. \quad (\text{A6})$$

The physical meaning of Eq. (A6) is that for  $\vec{E} = 0$ , a nonzero  $g$  will not have an exponential decay, as it does with Eq. (5), but a more complicated one. The actual form of  $g$  entails a microscopic calculation, which is well beyond the present discussion, but it is worth noting that microscopic quantum transport calculations often do lead to Boltzmann-type equations. Here the Boltzmann equation is a simple means to obtain a generalized Drude form of  $\bar{\epsilon}$  which will be causal.

For  $\vec{E} = \vec{E}_0 e^{-i\omega t}$  it is straightforward to solve for  $g_{\mathbf{k}}$ , and compute the current to find the conductivity

and dielectric constant. For cubic symmetry  $\bar{\epsilon}$  is given by

$$\bar{\epsilon}(\omega) = -\omega_p^2/\omega[\omega + iG(\omega)], \quad (\text{A7})$$

where, as usual,

$$\omega_p^2 = \frac{e^2}{3\pi^2\hbar} \int v dS_F \quad (\text{A8})$$

and

$$G(\omega) = \int_{-\infty}^{\infty} g(x)e^{i\omega x} dx \equiv R(\omega) + iI(\omega). \quad (\text{A9})$$

$G(\omega)$  appears in place of  $1/\tau$  and will, in general be complex, with its real and imaginary parts satisfying Kramers-Kronig relations because  $g(x) = 0$  for  $x < 0$ . Therefore,  $\bar{\epsilon}$  will also be causal, as it should. The form of Eq. (A7) is like that discussed by Mori,<sup>20</sup> in his very general work on transport coefficients, which suggests that the form has validity more general than the Boltzmann-equation approach used here to obtain it. This form has also been obtained by Allen<sup>21</sup> in an explicit treatment of electron-phonon scattering. Since  $g(x)$  is real,  $R$  is even in  $\omega$ , and  $I$  is odd in  $\omega$ . Therefore, for small enough  $\omega$ , and analytic  $g(\omega)$ ,  $R$  will be quadratic in  $\omega$  and  $I$  will be linear in  $\omega$ . The simple Drude case is recovered if  $g(x) = (1/\tau)\delta(x)$ , for then  $G(\omega) = 1/\tau$ , constant and real.

The quantities  $\tau_{\text{eff}}$  and  $\omega_{\text{eff}}^2$  of equations (A2) and (A3) can be found from Eq. (A7), in terms of the real and imaginary parts of  $G(\omega) = R(\omega) + iI(\omega)$ , the result being

$$\frac{1}{\tau_{\text{eff}}} = \frac{R}{1 - I/\omega}, \quad (\text{A10a})$$

$$\omega_{\text{eff}}^2 = \frac{\omega_p^2}{1 - I/\omega}. \quad (\text{A10b})$$

Thus,  $\omega_p^2$  acquires a frequency dependence associated with the same microscopic processes that render  $\tau$  frequency dependent. If  $I/\omega$  is small or constant in the frequency range of interest,  $\omega_p^2$  is constant, and then the two methods of finding  $\tau_{\text{eff}}$  mentioned at the outset of the discussion are approximately the same, amounting to finding  $R(\omega)$ . [The possibility of a constant  $I/\omega$  is fairly good, since  $I$  must be odd in  $\omega$ , and hence will be linear in  $\omega$  for small  $\omega$ , and  $g(\omega)$  analytic.] But in general, fitting  $\tau$  to  $\epsilon_2$  for constant  $\omega_p^2$  is inappropriate, and Eq. (A2) must be augmented by Eq. (A3). Also the quantities  $R$  and  $I$  are more closely related to microscopic theory and should be deduced from data in preference to  $\tau_{\text{eff}}$  and  $\omega_{\text{eff}}^2$ . The spectral shape of  $R$  can be obtained from the relation

$$R(\omega)/\omega_p^2 = (1/\tau_{\text{eff}})(1/\omega_{\text{eff}}^2). \quad (\text{A11})$$

The value of  $\omega_p^2$  cannot separately be deduced, since

it is mixed with  $I(\omega)$  in  $\omega_{\text{eff}}^2$  at all frequencies.

The quantity  $R(\omega)$  is related to, although not exactly the same as, the relaxation rate  $W$  of an electron at energy  $\hbar\omega$  above the Fermi energy. By examining  $W$  for a number of processes, Hopfield<sup>3</sup> has shown that  $R$  might often have the form

$$R(\omega) = a + b\omega^2. \quad (\text{A12})$$

The  $\omega^2$  dependence in Eq. (A12) arises from density-of-states effects.

Contact can also be made between the form of Eq. (A7) and schemes for fitting intraband data with an  $\bar{\epsilon}$  composed of sums of Drude terms and/or oscillators. For any  $G(\omega)$  the poles of  $\bar{\epsilon}$  can be found (in principle) and a partial fraction expansion of  $\bar{\epsilon}$  can be made, or inversely, for any  $\bar{\epsilon}$ ,  $G(\omega)$  can be found. As an example, if

$$\mathcal{G}(x) = G_0\delta(x) + G_1e^{-\alpha x}\Theta(x), \quad (\text{A13})$$

then

$$G(\omega) = G_0 + G_1/(\alpha - i\omega). \quad (\text{A14})$$

Putting Eq. (A14) into Eq. (A7), it is found that  $\bar{\epsilon}$  takes the form of a sum of two Drude terms

$$\bar{\epsilon} = \frac{-\omega_{p_1}^2}{\omega(\omega + i/\tau_1)} + \frac{-\omega_{p_2}^2}{\omega(\omega + i/\tau_2)} \quad (\text{A15})$$

if  $\omega_p^2$ ,  $G_0$ ,  $G_1$  and  $\alpha$  are chosen as

$$\omega_p^2 = \omega_{p_1}^2 + \omega_{p_2}^2,$$

$$\alpha = \frac{(\omega_{p_1}^2/\tau_2) + (\omega_{p_2}^2/\tau_1)}{\omega_{p_1}^2 + \omega_{p_2}^2},$$

$$G_0 = \frac{\omega_{p_1}^2/\tau_1 + \omega_{p_2}^2/\tau_2}{\omega_{p_1}^2 + \omega_{p_2}^2}, \quad (\text{A16})$$

$$G_1 = \frac{-\omega_{p_1}^2\omega_{p_2}^2(1/\tau_1 - 1/\tau_2)^2}{(\omega_{p_1}^2 + \omega_{p_2}^2)^2}.$$

Putting  $\mathcal{G}$  from Eq. (A13) into Eq. (A6), and combining with Eq. (A4) for  $\vec{E}=0$ , gives an integral

equation for the decay of  $g_{\vec{k}}$ , which is satisfied by

$$g_{\vec{k}} = Ce^{s_1 t} + De^{s_2 t}, \quad (\text{A17a})$$

with

$$s_{1,2} = \frac{1}{2}\{-(\alpha + G_0) \pm [(\alpha + G_0)^2 - 4(G_0 + G_1)]^{1/2}\} \\ = \begin{cases} -1/\tau_1, \\ -1/\tau_2. \end{cases} \quad (\text{A17b})$$

Thus, the two-carrier model of Eq. (A15) can be regarded as arising from a double-relaxation process of  $g_{\vec{k}}$  (two different scattering mechanisms), rather than two sets of carriers. The interpretation to be applied must be derived from the situation at hand. There probably are cases where Eq. (A15) genuinely arises from two sets of carriers.<sup>22</sup> In Ref. 22 it is pointed out that if certain inequalities hold among  $\omega_{p_1}$ ,  $\omega_{p_2}$ ,  $\tau_1$ ,  $\tau_2$ , the two-carrier model of Eq. (A15) leads to an  $\omega^2$  dependent of  $1/\tau_{\text{eff}}$ . In the present treatment, Eq. (A14) shows that for the single condition  $\omega/\alpha \ll 1$ ,  $R(\omega)$  has an  $\omega^2$  dependence:

$$R(\omega) = G_0 + \frac{\alpha G_1}{\alpha^2[1 + \omega^2/\alpha^2]} \\ \cong \left(G_0 + \frac{G_1}{\alpha}\right) + \frac{|G_1|}{\alpha^3} \omega^2. \quad (\text{A18})$$

The values of  $\omega_p^2$ ,  $\alpha$ ,  $G_0$ , and  $G_1$  can be chosen other than as in Eq. (A16), so that  $s_{1,2}$  of Eq. (A17b) can be complex, yielding oscillating decay of  $g_{\vec{k}}$  and an  $\bar{\epsilon}$  which can no longer be written as two Drude terms. Other forms of  $\mathcal{G}(x)$  lead to a more complicated  $\bar{\epsilon}$ . As a warning, it is clear that the form of  $\bar{\epsilon}$  in Eq. (A7) is so general that it can be inappropriately used to describe processes, such as interband transitions, that are completely outside the context in which Eq. (A7) was obtained. Therefore, this scheme must be used with discretion.

<sup>1</sup>Tu Chen, W. Stutius, J. W. Allen, and G. R. Stewart, AIP Conf. Proc. **29**, 532 (1976).

<sup>2</sup>J. W. Allen and W. Stutius, Solid State Commun. **20**, 561 (1976).

<sup>3</sup>J. J. Hopfield, AIP Conf. Proc. **4**, 358 (1972).

<sup>4</sup>J. B. Goodenough, *Progress in Solid State Chemistry*, edited by H. Reiss (Pergamon, Oxford, 1971), Vol. 5, p. 145.

<sup>5</sup>N. F. Mott, *Metal-Insulator Transitions* (Taylor and Francis, London, 1974).

<sup>6</sup>C. Herring, in *Magnetism*, Vol. IV, edited by G. T. Rado and H. Suhl (Academic, New York, 1966), p. 128.

<sup>7</sup>M. B. Stearns, Phys. Rev. B **8**, 4383 (1973).

<sup>8</sup>K. S. Liang and Tu Chen, Bull. Am. Phys. Soc. **21**, 440 (1976).

<sup>9</sup>H. Ehrenreich, in *Optical Properties and Electronic Structure of Metals and Alloys*, edited by F. Abelès (Wiley, New York, 1966), p. 115.

<sup>10</sup>J. W. Allen, J. C. Mikkelsen, and R. Allen, Physica (Utr.) B (to be published).

<sup>11</sup>J. Feinleib and B. Feldman, Rev. Sci. Instrum. **38**, 32 (1967).

<sup>12</sup>R. S. Bauer, W. E. Spicer, J. J. White III, J. Opt. Soc. Am. **64**, 830 (1974).

<sup>13</sup>We are indebted to G. Lucovsky for the use of his programs.



- <sup>14</sup>M. Thèye, Phys. Rev. B 2, 3060 (1970).
- <sup>15</sup>P. B. Johnson and R. W. Christy, Phys. Rev. B 9, 5056 (1974).
- <sup>16</sup>G. Thornton, A. F. Orchard, C. N. R. Rao, J. Phys. C 9, 1991 (1976).
- <sup>17</sup>P. M. Raccach and J. B. Goodenough, Phys. Rev. 155, 932 (1967).
- <sup>18</sup>A. P. Lenham, J. Opt. Soc. Am. 57, 473 (1967).
- <sup>19</sup>J. M. Ziman, *Principles of the Theory of Solids*, 2nd ed. (Cambridge U.P., Cambridge, England, 1972), p. 279.
- <sup>20</sup>H. Mori, Prog. Theor. Phys. 34, 399 (1965).
- <sup>21</sup>P. B. Allen, Phys. Rev. B 3, 305 (1971).
- <sup>22</sup>S. R. Nagel and S. E. Schnatterly, Phys. Rev. B 9, 1299 (1974).